C^1 and G^1 continuous rational motions using a conformal geometric algebra

Ben Cross, Robert J. Cripps

School of Mechanical Engineering, University of Birmingham, Birmingham, UK

Glen Mullineux*

Department of Mechanical Engineering, University of Bath, Bath, UK

Abstract

Traditional rational motion design describes separately the translation of a reference point in a body and the rotation of the body about it. This means that there is dependence upon the choice of reference point. When considering the derivative of a motion, some approaches require the transform to be unitary. This paper resolves these issues by establishing means for constructing free-form motions from specified control poses using multiplicative and additive approaches. It also establishes the derivative of a motion in the more general non-unitary case. This leads to a characterization of the motion at the end of a motion segment in terms of the end pose and the linear and angular velocity and this, in turn, leads to the ability to join motion segments together with either C^1- or G^1-continuity.

Keywords: Motion design, geometric algebra, geometric continuity, rational motion, quaternions, dual quaternions

1. Introduction

Techniques in computer aided geometric design (CAGD) for handling free-form curves are relatively mature when compared with free-form rigid-body motion design. Take for example the concept of geometric continu-

*Corresponding author

Email address: g.mullineux@bath.ac.uk (Glen Mullineux)

ity which has been employed to interpolate important geometric information, eliminating parameterization-dependent features, improving the overall shape characteristics of fitted curves [1, 2]. Similar concepts are now being applied to rigid-body motion design [3]. However many of these approaches have undesirable shortcomings.

Rigid-body motion design requires the definition of an object's position as well as its orientation in space. Early techniques used homogeneous 4×4 transformation matrices for this purpose [4]. Constructing a motion passing between two rigid-body transforms requires the development of interpolation techniques between matrices. Linear interpolation is not possible, due to the property that these matrices are not closed under addition, and hence other techniques have had to be developed [5, 6].

An approach different to matrices, using quaternions to represent rotations, has been established [7]. By considering rotation and translation separately, linear methods, and later derivative interpolation methods, have been developed yielding a rational representation for motions. More recently, parameterization independent motions have been produced [3]. Such interpolation however is dependent on coordinates, through a possibly ambiguous choice for the reference point with which to define the centre of rotation [8].

In a seminal paper on rigid-body motion design, Röschel [9] identified three desirable features. Basis functions for the rigid-body transformations should be rational functions (here referred to as rational motions) and indicated how a representation using dual quaternions can be obtained. Dual quaternions are now widely used in representing motions [10, 11, 12, 13, 14]. Secondly, interpolation should be Euclidean displacement invariant, that is it should be independent of the coordinates: an equivalent definition based on coordinate invariance is also available [15]. Thirdly, motion construction should be invariant with respect to the parameterization, an idea analogous to that of geometric continuity with curves [16].

Using dual quaternions and geometric algebra, it is possible to combine rotational and translational information. Dual quaternions are equivalent to an even-grade subalgebra of a larger geometric algebra. Furthermore, linear interpolations of these even-grade elements have an additional property of coordinate invariance. Derivative interpolation however requires an additional level of complexity.

Many derivative interpolation techniques that use geometric algebra require the even-grade elements to be "unitary" [16]. Additional complexity is thus required to insist that the results of interpolation through combi-

nations of even-grade elements remain unitary. Using geometric algebra, a distinction appears between the use of *multiplicative* and *additive* combinations. Multiplicative combinations preserve the unitary form of the results, whereas additive combinations, by themselves, do not.

Multiplicative operations over the unitary even-grade elements form a Lie group, $SE(3)$, and derivative interpolation can be achieved with consideration of its Lie algebra, $se(3)$, through exponential and logarithmic operations [6]. This increases the complexity of a representation and differs from traditional curve design, such as Bézier and B-spline curves, which are generated through repeated additive combinations of control points. Furthermore this representation does not admit a desirable rational polynomial basis.

Recent research has shown that free-form motions can be constructed through additive combinations of even-grade elements [17] and end-conditions for such additive motions have been investigated geometrically [18]. Many of the existing techniques from curve design, such as interpolation, naturally move over into motion design. However a theory for motion derivative interpolation, using additive combinations, has not been presented. This paper addresses this issue by establishing a framework for derivative interpolation on non-unitary even-grade elements. To begin, the theoretical foundations of derivative motion interpolation using geometric algebra are presented. The restriction that elements must be unitary is relaxed, enabling derivative interpolation using additive motions. Furthermore the familiar CAGD notion of geometric continuity, through parameter invariance, is derived. This results in new techniques for derivative interpolation using rational motion design, improving upon existing techniques, with the additional desirable property of coordinate invariance.

A recent publication [8] has considered C^1-continuous coordinate invariant rigid-body interpolation using the multiplicative approach. The purpose of this paper is to investigate similar results for multiplicative motions through an independent approach using geometric algebra, and to generalize beyond the multiplicative case so eliminating the requirement of using exponential and logarithmic expressions, yielding true polynomial rational motions in the additive case (without any unitary requirement). Motions are considered as varying rigid-body transforms of the whole of the moving body, thus removing any dependence upon the choice of a reference point in the body.

The next section presents the mathematical preliminaries for motion representation using geometric algebra, based on the conformal geometric alge-

bra (CGA) [19]. It is shown how even-grade elements in the algebra can be used to generate linear transforms of projective and Euclidean space. Conditions under which two even-grade elements generate the same transform are identified.

A variable even-grade element generates a variable transform which when applied to a body creates a motion. Section 3 considers the linear and angular velocities of the body. This leads to the idea of the velocity bivector, and to its extension in the non-unitary case, the velocity indicatrix.

In Section 4, motions are constructed from control poses using the de Casteljau algorithm in both the multiplicative and additive cases. Means for finding the derivatives of such motions are obtained. The approach does not assume that the motion is unitary. This leads to conditions for first order continuity (both C^1 and G^1) between motion segments and these represent the main results of the paper.

Section 5 demonstrates applications of the theory through examples. The first compares the multiplicative and additive motion segments determined by a given set of end conditions. The second considers the effect of changing the "shape factors" (as might be done with G^1-continuity) for a planar motion. The third considers the construction of a motion through a given set of precision poses using Hermite interpolation with cubic motion segments.

Finally, some conclusions are drawn. The contribution of this work is that conditions are established for joining together motion segments with C^1- and G^1-continuity. Parameters (shape factors) which can be freely chosen are identified. While other researchers have considered these issues for multiplicative motions, the results for additive motions are new. They require the introduction of the velocity indicatrix as a generalization of the concept of the velocity bivector. The significance of these ideas is that they allow free-form motion design to be undertaken with the additive form which is inherently computationally less demanding than the multiplicative form.

2. Geometric algebra

There are various forms of geometric algebra which have been investigated in the literature [20, 21, 22]. As it is widely used, the presentation here is based on the conformal geometric algebra (CGA) [19]. This is formed by starting with a real vector space with five basis vectors labelled: e_0, e_1, e_2, e_3, e_∞.

This is extended to a space of dimension 32 whose basis elements are e_σ where σ is an ordered subset of the set $\{0, 1, 2, 3, \infty\}$ of subscripts. The typical element of the algebra is then a linear combination of the form

$$a \;=\; \sum_\sigma a_\sigma \, e_\sigma \tag{1}$$

where the a_σ are real coefficients.

A multiplication on the space is defined in stages. Firstly e_σ is given as

$$e_\sigma \;=\; \prod_{i \in \sigma} e_i$$

where the product is in the order in which the subscripts appear in the ordered subset σ. Secondly, the product of two different basis vectors is defined by

$$-e_j e_i \;=\; e_i e_j \;=\; e_{ij} \qquad \text{for } \; i < j \; \text{ and } \; \{i, j\} \neq \{0, \infty\},$$

and, in the exceptional case, by

$$e_\infty e_0 \;=\; -2 - e_0 e_\infty \;=\; -2 - e_{0\infty}. \tag{2}$$

The squares of the basis vectors are defined by the following

$$e_1^2 = e_2^2 = e_3^2 = 1, \qquad e_0^2 = e_\infty^2 = 0.$$

Finally the product of two elements of the form of (1) is obtained by forming the sum of all products between the two sets of summands.

The basis element corresponding to the empty subset acts as a unity element for the multiplication and is identified with the real number 1: $e_\varnothing = 1$.

The *grade* of a basis element e_σ is the size of the subset σ. If the coefficients in the expression for a in (1) are zero except for basis elements of a particular grade, then that is also the grade of the element a. Thus an element of grade 1, that is a *vector*, is a linear combination of e_0, e_1, e_2, e_3, e_∞. A *bivector* is an element of grade 2. The idea extends to saying that an element has odd or even grade.

The *reverse* of a basis element is obtained by reversing the order of its subscripts. The reverse of general element is obtained by reversing all the

basis elements in (1). The reverse is denoted by an over-bar. Thus, for example,

$$\begin{aligned} \overline{e_{12}} &= e_2 e_1 = -e_{12} \\ \overline{e_1 + e_{123} + 2e_{0123\infty}} &= e_1 - 5e_{123} + 2e_{0123\infty}. \end{aligned}$$

An *inner product* and an *outer product* are defined as follows [17] for any elements x and y

$$\begin{aligned} x \cdot y &= \tfrac{1}{2}(xy + yx) \\ x \wedge y &= \tfrac{1}{2}(xy - yx). \end{aligned}$$

With this notation, the exceptional case of (2) can be rewritten as

$$e_0 \cdot e_\infty = -1.$$

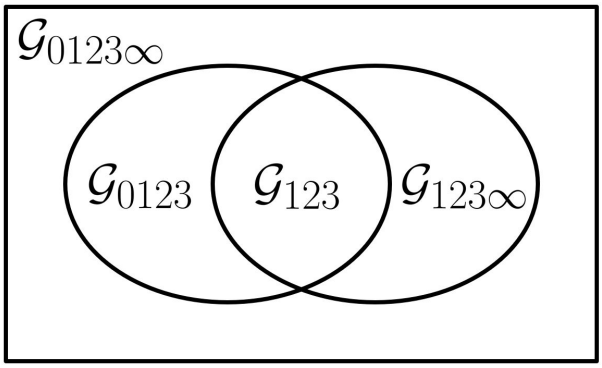

Figure 1: Subalgebras of $\mathcal{G}_{0123\infty}$

There are certain subalgebras which are identified: $\mathcal{G}_{123}$ is the one generated by e_1, e_2, e_3; $\mathcal{G}_{0123}$ is the one generated by e_0 and the elements of $\mathcal{G}_{123}$; similarly $\mathcal{G}_{123\infty}$ is generated by e_∞ and $\mathcal{G}_{123}$. In the same vein, $\mathcal{G}_{0123\infty}$ is used to denote the full algebra. These subalgebras are illustrated in Fig. 1. Additionally a superscript of a plus sign on any of these subalgebras denotes the subalgebra of even-grade elements within it. Thus $\mathcal{G}^+_{123}$ is the subalgebra of all combinations of the form

$$a_{12}e_{12} + a_{13}e_{13} + a_{23}e_{23}.$$

One particular basis element of $\mathcal{G}_{0123\infty}$ is given special notation

$$\omega \;=\; e_{123\infty} \quad \in \mathcal{G}_{123\infty},$$

and it has the following properties

$$\omega^2 = 0, \qquad \overline{\omega} = \omega.$$

Three-dimensional Euclidean space $\mathbb{R}^3$ can be regarded as lying within $\mathcal{G}_{123}$ by use of the correspondence

$$\mathbf{a} \;=\; (a_1, a_2, a_3) \;\longleftrightarrow\; a_1 e_1 + a_2 e_2 + a_3 e_3. \tag{3}$$

With this correspondence and using bold letters to denote vectors in $\mathbb{R}^3$ the following result relates the above outer product in $\mathcal{G}_{123}$ to the vector product of three-dimensional space [17].

Lemma 2.1. *With the correspondence (3), for* $\mathbf{a}, \mathbf{b} \in \mathbb{R}^3$*,*

$$\mathbf{a} \times \mathbf{b} \;\longleftrightarrow\; -(a \wedge b) e_{123}.$$

To be able to deal with (projective) geometry, there is a need to embed the projective space $\mathbb{RP}^3$ into the geometric algebra [17]. This is achieved with the map $E : \mathbb{RP}^3 \to \mathcal{G}_{0123}$ given by

$$E : (W, X, Y, Z) \mapsto \begin{cases} X e_1 + Y e_2 + Z e_3 & \text{if} \quad W = 0 \\ e_0 + (X/W) e_1 + (Y/W) e_2 + (Z/W) e_3 & \text{if} \quad W \neq 0 \end{cases}$$

and there is a similar map $E : \mathbb{R}^3 \to \mathcal{G}_{0123}$ given by

$$E : (x, y, z) \mapsto e_0 + x e_1 + y e_2 + z e_3.$$

A projection map [17] $P : \mathcal{G}_{0123\infty} \to \mathbb{RP}^3$ is defined by

$$P : a = \sum_\sigma a_\sigma e_\sigma \mapsto (a_0, a_1, a_2, a_3)$$

and a similar map $P : \mathcal{G}_{0123\infty} \to \mathbb{R}^3$ is given by

$$P : a = \sum_\sigma a_\sigma e_\sigma \mapsto (a_1/a_0, a_2/a_0, a_3/a_0)$$

assuming that a_0 is non-zero.

If $S \in \mathcal{G}^+_{123\infty}$ is an even-grade element, then a map f_S of $\mathcal{G}_{0123\infty}$ to itself is defined by

$$f_S : x \mapsto \overline{S}xS.$$

If x is a vector, then $f_S(x)$ has odd grade. It follows [17] that the composition

$$F_S = P f_S E$$

is a map from $\mathbb{RP}^3$ to itself, and it can be restricted to a map of $\mathbb{R}^3$ to itself; F_S and its restriction are rigid-body transforms. The form of $\overline{S}xS$ is required for later work and is given by the following result. It can be proved by multiplying out the various terms. As this is not in itself very illuminating, the proof is given separately in the appendix 1.

Lemma 2.2. *(i) If $S \in \mathcal{G}^+_{123\infty}$ is an even-grade element and $x \in \mathcal{G}_{0123\infty}$ is a vector, then $\overline{S}xS$ takes the form*

$$\overline{S}xS \;=\; v + \lambda\sigma$$

where v is a vector, λ is a real number, and

$$\sigma \;=\; e_0 \cdot \omega \;=\; -e_{123} + e_{0123\infty}.$$

(ii) The product $\overline{S}S$ has the form $\alpha + \beta e_{123\infty}$, where α, β are real numbers, and the coefficient of e_0 in $\overline{S}xS$ is α times the coefficient of e_0 in x.

(iii) Further, σ commutes with every element of $\mathcal{G}_{0123\infty}$ so that equivalently $\sigma \wedge x = 0$ for all $x \in \mathcal{G}_{0123\infty}$.

The term *transform* is now used to refer to the linear transform of $\mathbb{RP}^3$ or $\mathbb{R}^3$ generated by a map of the form F_S for $S \in \mathcal{G}^+_{123\infty}$.

Since

$$\overline{(UV)}x(UV) \;=\; \overline{V}(\overline{U}xU)V,$$

the following result follows.

Lemma 2.3. *For $U, V \in \mathcal{G}^+_{123\infty}$, $F_{UV} = F_V\, F_U$.*

If $a \in \mathcal{G}_{123}$ is a unit vector (that is one whose length $\sqrt{[\overline{a}a]}$ is unity), and $b = ae_{123} \in \mathcal{G}_{123}$ is the corresponding unit bivector, then the element

$$R \;=\; (\cos\tfrac{1}{2}\phi) + (\sin\tfrac{1}{2}\phi)b \in \mathcal{G}_{123} \subset \mathcal{G}_{123\infty}$$

generates a transform F_R which is a rotation of $\mathbb{R}^3$ through angle ϕ about an axis through the origin in the direction of a.

Similarly, if $v \in \mathcal{G}_{123}$ is a vector then the element

$$T \;=\; 1 + \tfrac{1}{2} v e_\infty \in \mathcal{G}_{123\infty}$$

generates a transform F_T which is a translation of $\mathbb{R}^3$ along the vector v.

Further, both R and T are *unitary* in the sense that

$$\overline{R}R \;=\; 1 \;=\; \overline{T}T.$$

Any element of the form

$$c = a + b\omega$$

where a and b are real coefficients is called a *pseudoscalar*. The set of all pseudoscalars is a subalgebra of $\mathcal{G}_{123\infty}$. The above pseudoscalar c is said to be *non-singular* if a is non-zero. The following result holds [17].

Lemma 2.4. *Suppose that $c = a + b\omega$ is a non-singular pseudoscalar. Then*

(i) c has a multiplicative inverse which is a non-singular pseudoscalar, namely $(a - b\omega)/(a^2)$;

(ii) if $a > 0$, then c has square roots which are non-singular pseudoscalars, namely $\pm(2a + b\omega)/(2\sqrt{a})$.

If $c \in \mathcal{G}_{123\infty}$ is a pseudoscalar, then it generates a transform F_c. The next result identifies what this transform is.

Lemma 2.5. *A pseudoscalar $c \in \mathcal{G}_{123\infty}$ generates a transform F_c. This is the identity transform if c is non-singular, and otherwise is the zero transform (that is, it maps everything to zero).*

Proof. Suppose that $c = a + b\omega$ and consider its action on a typical vector $v = e_0 + d \in \mathcal{G}_{0123}$ where $d \in \mathcal{G}_{123}$:

$$\begin{aligned}
\overline{c}vc &= (a + b\omega)v(a + b\omega) \\
&= (a + b\omega)(av + bv\omega) \\
&= a^2 v + ab(v\omega + \omega v) + b^2 \omega v \omega \\
&= a^2 v + 2ab(v \cdot \omega) + b^2 \omega e_0 \omega \\
&= a^2 v + 2ab(v \cdot \omega) + 2b^2 e_\infty \\
&= a^2 v + 2ab(e_0 \cdot \omega) + 2b^2 e_\infty \\
&= a^2 v + 2ab(e_{0123\infty} - e_{123}) + 2b^2 e_\infty
\end{aligned}$$

since $d \cdot \omega = 0 = \omega d\omega$. Hence

$$P(\overline{c}vc) \;=\; a^2 v.$$

If a is non-zero, then $a^2 v$ is projectively equivalent to v and the transform is the identity. If $a = 0$, then it is the zero transform. $\square$

The typical element $S \in \mathcal{G}^+_{123\infty}$ has the form

$$S = S_\varnothing + S_{12}e_{12} + S_{13}e_{13} + S_{23}e_{23} + S_{1\infty}e_{1\infty} + S_{2\infty}e_{2\infty} + S_{3\infty}e_{3\infty} + S_\omega\omega. \quad (4)$$

By multiplying out, it is seen that

$$\overline{S}S = (S_\varnothing^2 + S_{12}^2 + S_{13}^2 + S_{23}^2) + 2(S_\varnothing S_\omega - S_{12}S_{3\infty} + S_{13}S_{2\infty} - S_{23}S_{1\infty})\omega \quad (5)$$

$$\begin{aligned}\overline{S}e_1S \;=\; & (S_\varnothing^2 - S_{12}^2 - S_{13}^2 + S_{23}^2)e_1 \\ & +2(S_\varnothing S_{12} - S_{13}S_{23})e_2 + 2(S_\varnothing S_{13} + S_{12}S_{23})e_3 \\ & +2(S_\varnothing S_{1\infty} + S_{12}S_{2\infty} + S_{13}S_{3\infty} + S_{23}S_\omega)e_\infty \end{aligned} \quad (6)$$

$$\begin{aligned}\overline{S}e_2S \;=\; & -2(S_\varnothing S_{12} + S_{13}S_{23})e_1 \\ & +(S_\varnothing^2 - S_{12}^2 + S_{13}^2 - S_{23}^2)e_2 + 2(S_\varnothing S_{23} - S_{12}S_{13})e_3 \\ & +2(S_\varnothing S_{2\infty} - S_{12}S_{1\infty} - S_{13}S_\omega + S_{23}S_{3\infty})e_\infty \end{aligned} \quad (7)$$

$$\begin{aligned}\overline{S}e_3S \;=\; & -2(S_\varnothing S_{13} - S_{12}S_{23})e_1 \\ & -2(S_\varnothing S_{23} + S_{12}S_{13})e_2 + (S_\varnothing^2 + S_{12}^2 - S_{13}^2 - S_{23}^2)e_3 \\ & +2(S_\varnothing S_{3\infty} + S_{12}S_\omega - S_{13}S_{1\infty} - S_{23}S_{2\infty})e_\infty \end{aligned} \quad (8)$$

and the vector part of the product $\overline{S}e_0S$ is given by

$$\begin{aligned}\mathrm{vec}(\overline{S}e_0S) \;=\; & (S_\varnothing^2 + S_{12}^2 + S_{13}^2 + S_{23}^2)e_0 \\ & +2(S_\varnothing S_{1\infty} - S_{12}S_{2\infty} - S_{13}S_{3\infty} + S_{23}S_\omega)e_1 \\ & +2(S_\varnothing S_{2\infty} + S_{12}S_{1\infty} - S_{13}S_\omega - S_{23}S_{3\infty})e_2 \\ & +2(S_\varnothing S_{3\infty} + S_{12}S_\omega + S_{13}S_{1\infty} + S_{23}S_{2\infty})e_3 \\ & +2(S_{1\infty}^2 + S_{2\infty}^2 + S_{3\infty}^2 + S_\omega^2)e_\infty. \end{aligned} \quad (9)$$

Here (5) shows that $\overline{S}S$ is a pseudoscalar in $\mathcal{G}^+_{123\infty}$. It is singular if and only if $S_\varnothing = S_{12} = S_{13} = S_{23} = 0$. In this case, (6), (7), (8), (9) show that $\mathrm{vec}(\overline{S}pS)$ is a scalar multiple of e_∞ for any vector $p \in \mathcal{G}_{0123}$. This becomes zero under the projection map P and so the map F_S generated by S is the zero transform.

Thus if S generates a non-zero transform, $\overline{S}S$ is non-singular and has a square root which is also a non-singular pseudoscalar. Set

$$|S| \;=\; \sqrt{[\overline{S}S]}.$$

Conversely, (9) shows that if S is non-singular, then S generates a non-zero transform.

Lemma 2.6. *For an element $S \in \mathcal{G}^+_{123\infty}$, $\overline{S}S$ is a pseudoscalar which is non-singular if and only if S generates a non-zero transform F_S. Further, if $\overline{S}S$ is non-singular, then*

(i) $U = S/|S| \in \mathcal{G}^+_{123\infty}$ is unitary and generates the same transform as S;

(ii) $V = \overline{S}/|S|^2$ is such that $SV = 1$ so that $V = S^{-1}$.

Proof. The various parts follow from the above discussion and Lemmas 2.3 and 2.5. □

Lemma 2.7. *If an element $S \in \mathcal{G}^+_{123\infty}$ generates the identity transform, then*

(i) S is a pseudoscalar;

(ii) if S is unitary, S is ± 1.

Proof. By Lemma 2.6(i), $S = \gamma U$ where γ is a pseudoscalar and U is unitary. Hence it is sufficient to prove part (ii), as part (i) then follows.

So assume S is unitary, so that from (5),

$$S_\varnothing^2 + S_{12}^2 + S_{13}^2 + S_{23}^2 \;=\; 1.$$

Consider $\overline{S}(e_0 + e_i)S$, for $i = 1, 2, 3$. From (6), (7), (8), (9), the coefficient of e_0 is unity in each case. Hence the coefficient of e_i is also unity in each case, so that

$$\begin{aligned} S_\varnothing^2 - S_{12}^2 - S_{13}^2 + S_{23}^2 \;&=\; 1 \\ S_\varnothing^2 - S_{12}^2 + S_{13}^2 - S_{23}^2 \;&=\; 1 \\ S_\varnothing^2 + S_{12}^2 - S_{13}^2 - S_{23}^2 \;&=\; 1. \end{aligned}$$

These three equations and the previous one show that

$$S_\varnothing^2 = 1, \qquad S_{12} = S_{13} = S_{23} = 0.$$

Consideration of the coefficient of ω in (5) shows that $S_\omega = 0$. Finally, consideration of the coefficients of e_1, e_2, e_3 in (9) shows that

$$S_{1\infty} = S_{2\infty} = S_{3\infty} = 0.$$

Hence $S = S_\varnothing = \pm 1$. □

A non-singular element $S \in \mathcal{G}^+_{123\infty}$ generates a transform F_S which acts on $\mathbb{R}^3$ as a rigid-body transform. A body is transformed by transforming all the points within it. This results in a new position and orientation of the body and this is called a *pose*. The term is also applied to the element S itself.

Suppose the pose S can change so that, for example, it is a function $S(t) \in \mathcal{G}^+_{123\infty}$ of some parameter t. Then as the parameter varies the pose of the body changes and the result is a *motion* of the body.

Two poses or two motions are said to be *equivalent* if one is the product of the other and a non-singular pseudoscalar: in the case of motions, the pseudoscalar is a function of the parameter. Since the pseudoscalar has a multiplicative inverse (Lemma 2.4), this is an equivalence relation.

Theorem 2.8. *Two poses or motions generate the same non-zero transforms of* $\mathbb{RP}^3$ *and* $\mathbb{R}^3$ *if and only if they are equivalent.*

Proof. If they are equivalent, then they generate the same transforms by Lemma 2.3 and 2.4.

Conversely, suppose $U, V \in \mathcal{G}_{123\infty}$ generate the same non-zero transforms. By Lemma 2.6, U has a multiplicative inverse. So by Lemma 2.3, if I is the identity transform, then

$$I \;=\; F_{U^{-1}} F_U \;=\; F_{U^{-1}} F_V \;=\; F_{VU^{-1}}.$$

By Lemma 2.7, $VU^{-1} = \gamma$ is a pseudoscalar, so that $V = \gamma U$, and U and V are equivalent. □

The next section considers the velocity associated with a motion.

3. Velocity bivector

Consider an odd-grade element of the form

$$r \;=\; r(t) \;=\; We_0 + Xe_1 + Ye_2 + Ze_3 + Ke_\infty + \lambda\sigma \;\in\; \mathcal{G}_{0123\infty}$$

where W, X, Y, Z, K, λ are functions of a parameter t which is regarded as time and $\sigma = e_0 \cdot \omega$ as in Lemma 2.2. Then, differentiating with respect to t,

$$\dot{r} \;=\; \dot{W}e_0 + \dot{X}e_1 + \dot{Y}e_2 + \dot{Z}e_3 + \dot{K}e_\infty + \dot{\lambda}\sigma.$$

After use of the projection map P, the element $r(t)$ represents a moving point with cartesian coordinates

$$\left(\frac{X}{W}, \frac{Y}{W}, \frac{Z}{W} \right).$$

In cartesian coordinates its velocity is

$$(v_1, v_2, v_3) = \left(\frac{W\dot{X} - \dot{W}X}{W^2}, \frac{W\dot{Y} - \dot{W}Y}{W^2}, \frac{W\dot{Z} - \dot{W}Z}{W^2} \right)$$

which is represented in $\mathcal{G}_{0123}$ by the vector

$$v \;=\; v_1e_1 + v_2e_2 + v_3e_3.$$

Since σ commutes with every element (Lemma 2.2), the following outer product holds

$$\begin{aligned} r \wedge \dot{r} \;=\; & (W\dot{K} - \dot{W}K) \\ & + (W\dot{X} - \dot{W}X)e_{01} + (W\dot{Y} - \dot{W}Y)e_{02} + (W\dot{Z} - \dot{W}Z)e_{03} \\ & + (W\dot{K} - \dot{W}K)e_{0\infty} \\ & + (X\dot{Y} - \dot{X}Y)e_{12} + (X\dot{Z} - \dot{X}Z)e_{13} + (Y\dot{Z} - \dot{Y}Z)e_{23} \\ & + (X\dot{K} - \dot{X}K)e_{1\infty} + (Y\dot{K} - \dot{Y}K)e_{2\infty} + (Z\dot{K} - \dot{Z}K)e_{3\infty} \end{aligned}$$

and gives the next result.

Lemma 3.1. *If a moving point is represented by*

$$r(t) \;=\; W(t)e_0 + X(t)e_1 + Y(t)e_2 + Z(t)e_3 + K(t)e_\infty + \lambda(t)\sigma \;\in\; \mathcal{G}_{0123\infty}$$

then

$$r \wedge \dot{r} \;=\; k \;+\; W(t)^2\, e_0\, v(t) \;+\; \mu e_{0\infty} \;+\; C(t) \tag{10}$$

where k, μ are scalars, $v(t) \in \mathcal{G}_{123}$ is the velocity of the point, and $C(t) \in \mathcal{G}_{123\infty}$ is a bivector.

Suppose that $S(t) \in \mathcal{G}^+_{123\infty}$ is an element generating non-zero transforms forming a motion of some body. By Lemma 2.6, it has an inverse. Define the *velocity indicatrix* as the following:

$$\Psi(t) \;=\; 2\,S(t)^{-1}\,\dot{S}(t). \tag{11}$$

Set

$$\begin{aligned}\nu &= \tfrac{1}{2}(\Psi - \overline{\Psi})\\ \gamma &= \tfrac{1}{2}(\Psi + \overline{\Psi})\end{aligned}$$

so that γ is the pseudoscalar part of the velocity indicatrix with (say) $\gamma = \alpha + \beta\omega$, and ν is its bivector part and is called the *velocity bivector*.

Suppose that $\hat{p}$ is a point fixed in the moving body, and $\hat{r}(t)$ is its image under $F_{S(t)}$. There are corresponding vectors

$$p = E(\hat{p}) \in \mathcal{G}_{0123}, \qquad r = r(t) = f_{S(t)}(p) \in \mathcal{G}_{0123\infty},$$

with

$$r(t) \;=\; \overline{S}pS.$$

In order to relate the motion of the point to the velocity indicatrix, the product $r \wedge \dot{r}$ is now considered with the aim of extracting the component of the form $e_0 v$ where $v \in \mathcal{G}_{123}$ so that Lemma 3.1 can be applied. Firstly $\dot{r}$ is considered.

Applying Lemma 2.2, as the transform is non-zero, $\overline{S}S$ is non-singular and the coefficient W of e_0 in $r(t)$ is non-zero, and r has the form

$$r \;=\; W(e_0 + q + \lambda e_\infty + \mu\sigma)$$

where λ, μ are real numbers, $q \in \mathcal{G}_{123}$ is a vector, and $\sigma = e_0 \cdot \omega$.

It is seen that

$$\overline{S}^{-1} r = pS, \qquad rS^{-1} = \overline{S}p$$

and

$$\begin{aligned}\dot{r} &= \overline{\dot{S}}pS \;+\; \overline{S}p\dot{S}\\ &= \overline{\dot{S}}\overline{S}^{-1} r \;+\; rS^{-1}\dot{S}\\ &= \tfrac{1}{2}\overline{\Psi} r \;+\; \tfrac{1}{2} r\Psi\\ &= \tfrac{1}{2}(\gamma - \nu) r \;+\; \tfrac{1}{2} r(\gamma + \nu)\\ &= \tfrac{1}{2}(\gamma r + r\gamma) + \tfrac{1}{2}(r\nu - \nu r)\\ &= (\gamma \cdot r) + (r \wedge \nu).\end{aligned}$$

Substituting for γ gives

$$\begin{aligned}\dot{r} &= \alpha r + \beta(\omega \cdot r) + (r \wedge \nu) \\ &= \alpha r + \beta W\sigma + \beta W\mu e_\infty + (r \wedge \nu). \end{aligned} \tag{12}$$

Next consider $r \wedge \nu$. As $\nu \in \mathcal{G}_{123\infty}$ is a bivector, it can be written as

$$\nu = ae_{123} + be_\infty$$

where $a, b \in \mathcal{G}_{123}$ are vectors. Hence, using Lemma 2.2 and noting that $e_0 \wedge (ae_{123}) = e_\infty \wedge (ae_{123}) = 0$,

$$\begin{aligned} r \wedge \nu &= W[e_0 \wedge (be_\infty) + q \wedge (ae_{123}) + q \wedge (be_\infty)] \\ &= W[b + \tfrac{1}{2}(qae_{123} - ae_{123}q) + \tfrac{1}{2}(qbe_\infty - be_\infty q)] \\ &= W[b + \tfrac{1}{2}(qae_{123} - aqe_{123}) + \tfrac{1}{2}(qbe_\infty + bqe_\infty)] \\ &= W[b + (q \wedge a)e_{123} + (q \cdot b)e_\infty]. \end{aligned}$$

Now consider $r \wedge \dot{r}$ and in particular its components of the form $e_0 v$ where $v \in \mathcal{G}_{123}$ is a vector. From (12)

$$r \wedge \dot{r} = \beta W\mu(r \wedge e_\infty) + r \wedge (r \wedge \nu).$$

Here in the first term on the right

$$\begin{aligned} r \wedge e_\infty &= W(e_0 \wedge e_\infty + q \wedge e_\infty) \\ &= W(1 + e_{0\infty} + qe_\infty) \end{aligned}$$

which has no component of the required form.

Since $r \wedge \nu$ does not involve e_0, the required component derived from the second term is the contribution from

$$\begin{aligned} & W^2 e_0 \wedge [b + (q \wedge a)e_{123} + (q \cdot b)e_\infty] \\ = \; & W^2 e_0[b + (q \wedge a)e_{123}] + W^2(q \cdot b)(e_0 \wedge e_\infty) \\ = \; & W^2 e_0[b + (q \wedge a)e_{123}] + W^2(q \cdot b)(1 + e_{0\infty}) \end{aligned}$$

and the second term on the right makes no contribution. Comparison of this with (10), allows the deduction that

$$v = b + (q \wedge a)e_{123} = \mathbf{b} + (\mathbf{a} \times \mathbf{q})$$

where the bold terms are regarded as vectors in $\mathbb{R}^3$ and use is made of Lemma 2.1.

With vectors in $\mathbb{R}^3$, if point A in a rigid body has velocity $\mathbf{v}_A$ then the velocity of another point B in the body is [23]

$$\mathbf{v}_B \;=\; \mathbf{v}_A \;+\; \mathbf{\Omega} \times \mathbf{r}_{BA} \tag{13}$$

where $\mathbf{\Omega}$ is the angular velocity of the body and $\mathbf{r}_{BA}$ is the position of B relative to A.

Comparing this with the previous equation gives the following result.

Theorem 3.2. *Suppose that $S(t)$ is a motion of a rigid body. Then its velocity bivector $\nu(t)$ and velocity indicatrix $\Psi(t)$ can be written as*

$$\begin{aligned} \nu(t) \;&=\; \Omega(t)e_{123} + u(t)e_\infty \\ \Psi(t) \;&=\; \gamma(t) + \nu(t) \end{aligned}$$

where $\gamma(t) \in \mathcal{G}_{123\infty}$ is a pseudoscalar, and $\Omega(t), u(t) \in \mathcal{G}_{123}$ are vectors.

Further, $\Omega(t)$ is the angular velocity of the body, $u(t)$ is the linear velocity of that point in the body instantaneously at the global origin, and the velocity v_Q of the point Q at the position (instantaneously, relative to global axes) $e_0 + q$ with $q \in \mathcal{G}_{123}$ is given by

$$v_Q \;=\; u + (q \wedge \Omega)e_{123}. \tag{14}$$

Proof. Most of this has already been established. The nature of u follows by taking $q = 0$ in (14), so that Q is (instantaneously) at the global origin. In this case, $u = v_Q$. □

The velocity bivector is an element with six components, three of which correspond to linear velocity and three to angular velocity. It corresponds to "twist" in space kinematics [24]. Appendix 2 gives the equivalent result for the velocity indicatrix when dual quaternions are used to represent motions.

Corollary 3.3. *Under the conditions of the Theorem 3.2, if a point is (instantaneously) at point $r \in \mathcal{G}_{123}$ relative to the global origin and has velocity v, then*

$$\nu \;=\; \Omega e_{123} + v e_\infty + (\Omega \wedge r)\omega.$$

Proof. The velocity of the point is related to the velocity of the point instantaneously at the origin by

$$\begin{aligned} \mathbf{v} &= \mathbf{u} + (\mathbf{\Omega} \times \mathbf{r}) \\ v &= u - (\Omega \wedge r) e_{123}. \end{aligned}$$

Substituting into the expression for $\nu(t)$ in the theorem completes the proof. □

There is the special case when a motion is unitary for all values of the parameter.

Lemma 3.4. *If $S(t)$ is a motion which is unitary for all values of t, then its velocity indicatrix is the same as its velocity bivector.*

Proof. If $\overline{S(t)}S(t) = 1$ for all t, then

$$S^{-1} = \overline{S}, \qquad \text{and} \qquad \overline{\dot{S}}S + \overline{S}\dot{S} = 0.$$

The velocity indicatrix is now $\Psi = 2\overline{S}\dot{S}$, and

$$\overline{\Psi} = 2\overline{\dot{S}}S = -2\overline{S}\dot{S} = -\Psi.$$

Hence $\Psi \in \mathcal{G}^+_{123\infty}$ is a bivector and so is the same as the velocity bivector. □

4. Motion construction

A motion can be created between given poses A and B by generating a function $S(t)$ which interpolates them. This function then generates a *motion segment* between the two poses. There are (at least) two ways in which this can be done. The first is the *slerp* (spherical linear interpolation) [7] construction given by

$$S(t) = \Phi(A, B; t) = A\,(\overline{A}B)^t \quad \text{for } 0 \le t \le 1. \tag{15}$$

If A and B are both unitary, then so is $S(t)$, and $S(0) = A$ and $S(1) = B$, so that the given poses are indeed interpolated.

If α and β are pseudoscalars, then these commute with even-grade elements of $\mathcal{G}_{123\infty}$ and so

$$\Phi(\alpha A, \beta B; t) = \alpha^{1+t}\beta^t A\,(\overline{A}B)^t = \alpha^{1+t}\beta^t \Phi(A, B; t). \tag{16}$$

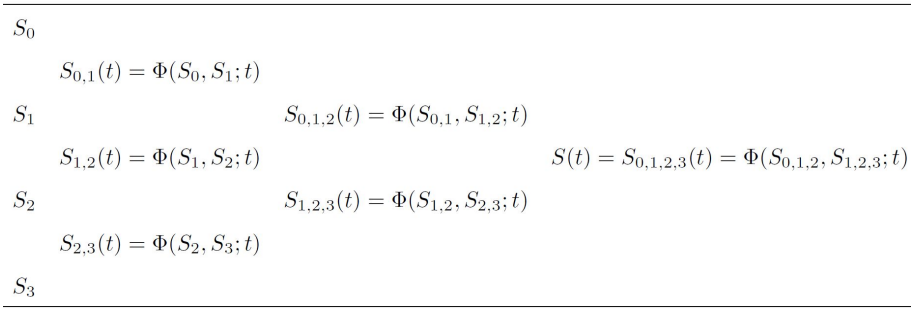

Figure 2: de Casteljau tableau starting with control poses S_0, S_1, S_2, S_3

which is a pseudoscalar times the motion in (15). By Lemmas 2.3 and 2.5 the actual transforms generated are the same, and so, by Lemma 2.6(i), A and B could be replaced by their unitary versions, although it is not necessary so to do. In general, $S(0)$ and $S(1)$ generate the same transform as A and B respectively and, in this sense, $S(t)$ is an interpolation of the two given poses.

The slerp construction is said to be *multiplicative* since this is form of (15). To evaluate the non-integer power, it is necessary to use the exponential and logarithm functions.

The other form of interpolation is *additive* and this is given by

$$S(t) = \Phi(A, B; t) = (1 - t)A + tB \quad \text{for} \quad 0 \leq t \leq 1. \tag{17}$$

Again $S(0) = A$ and $S(1) = B$. Since non-integer powers are avoided, (17) is easier to deal with. However, since the corresponding transform becomes the zero transformation if $S(t)$ becomes a singular pseudoscalar, it either needs to be assumed that this does not happen or special steps taken if it does occur.

Both (15) and (17) represent motions which are the combination of a pair of poses A and B. Using the de Casteljau algorithm [25] and starting with four control poses S_0, S_1, S_2, S_3, the tableau shown in Fig. 2 is formed, in which each new entry is a pairwise combination of the two terms to its left.

More generally, starting with $n+1$ poses, S_i, for $0 \leq i \leq n$, and using the additive combination results in the familiar Bézier combination of degree n

[25],

$$S(t) \;=\; \sum_{i=0}^{n} \binom{n}{i} S_i \, (1-t)^{n-i} \, t^i. \tag{18}$$

This is an additive Bézier motion. The result of combining $n+1$ poses using the multiplicative combination is also said to have *degree* n: the result is of course far from being a polynomial but is nonetheless called a multiplicative Bézier motion.

By introducing knots, it is straightforward to generate additive and multiplicative B-spline motions with the de Casteljau algorithm by extension of the construction of B-spline curves [25]. However, for brevity only Bézier motions are considered here.

Note that the motions constructed here are in terms of a variable rigid-body transform for the whole body. An alternative (perhaps more common) approach is to define a motion in terms of the (translational) path traced by a specific reference point in the body and the (rotational) motion of the body about that point (cf. Jaklič et al. [3] Počkaj [26], Krajnc [27]). This has the potential disadvantage that the motion is dependent upon the choice of reference point: if a different point for a given motion is selected then its path is not necessarily of the same form as the original. Working with the transform of the whole body means that there is no reference point (and hence no dependency).

Lemma 4.1. *If $S(t)$ is the multiplicative motion generated by a set of control poses, then the motion generated by a set of equivalent control poses is equivalent to the original motion and hence generates the same transform.*

Proof. Repeated use of (16) shows that each entry in the tableau with the new control poses is simply a pseudoscalar times the corresponding entry in the tableau for the original motion. Hence the new motion itself is a pseudoscalar times the original motion and so is equivalent to it. Theorem 2.8 shows that the new motion creates the same transform. □

In order to be able to join motion segments together smoothly, it is necessary to know the derivative of a motion at the ends of its segment. This is straightforward and well-known for an additive Bézier segment as in (18).

Lemma 4.2. *If $S(t)$ is the additive Bézier motion of degree n defined by the control poses S_i, for $0 \le i \le n$, then*

$$\dot{S}(0) \;=\; n(S_1 - S_0),$$

and hence

$$S(t) = S(0) + nt(S_1 - S_0) + O(t^2).$$

The following two lemmas deal with what happens for a multiplicative Bézier segment: this is complicated by the fact that the multiplication is not commutative.

Lemma 4.3. *For non-singular elements $X, Y \in \mathcal{G}^+_{123\infty}$ and a real parameter t*

$$[X + tY]^t \;=\; 1 + t\log(X) + O(t^2).$$

Proof. Using Lemma 2.6,

$$\begin{aligned}
[X + tY]^t &= \exp[t\log(X + tY)] \\
&= 1 + t\log(X + tY) + O(t^2) \\
&= 1 + t\log X + t\log(1 + tX^{-1}Y) + O(t^2) \\
&= 1 + t\log X + O(t^2).
\end{aligned}$$

□

Lemma 4.4. *If $S(t)$ is the multiplicative Bézier motion of degree n defined by the control poses S_i, for $0 \le i \le n$, then*

$$S(t) \;=\; S_0[1 + nt\log(\overline{S_0}S_1)] + O(t^2).$$

Proof. Define the following two functions

$$\begin{aligned}
\Phi^{(0)}_k(t) &= \Phi(S_{0,1,\ldots,k-1}, S_{1,2,\ldots,k}; t) \\
\Phi^{(1)}_k(t) &= \Phi(S_{1,2,\ldots,k}, S_{2,3,\ldots,k+1}; t)
\end{aligned}$$

so that the $\Phi^{(0)}_k$ are the functions along the topmost sloping row of the de Casteljau tableau, and the $\Phi^{(1)}_k$ are those of the next sloping row.

The lemma is proved if it can be shown that

$$\Phi^{(0)}_k(t) \;=\; S_0[1 + kt\log(\overline{S_0}S_1) + O(t^2)] \tag{19}$$

for all k with $1 \le k \le n$.

The proof is by induction on k. In the case when $k = 1$,

$$\Phi^{(0)}_1(t) \;=\; \Phi(S_0, S_1; t) \;=\; S_0(\overline{S_0}S_1)^t$$

and then, by Lemma 4.3 (with $Y = 0$),

$$\Phi_1^{(0)}(t) = S_0[1 + t\log(\overline{S_0}S_1) + O(t^2)]$$

which is (19) in this case.

So now assume that (19) holds for k and prove it for $k+1$.

Since $\Phi_k^{(1)}(t)$ is defined by a tableau based on a sequence of control poses starting with S_1, the inductive hypothesis says that also

$$\Phi_k^{(1)}(t) = S_1[1 + kt\log(\overline{S_1}S_2) + O(t^2)]$$

and then

$$\begin{aligned}\overline{\Phi_k^{(0)}(t)}\Phi_k^{(1)}(t) &= [\overline{(1 + kt\log(\overline{S_0}S_1))}\overline{S_0} + O(t^2)][S_1(1 + kt\log(\overline{S_1}S_2)) + O(t^2)] \\ &= \overline{S_0}S_1 + O(t)\end{aligned}$$

so that

$$[\overline{\Phi_k^{(0)}(t)}\Phi_k^{(1)}(t)]^t = 1 + t\log(\overline{S_0}S_1) + O(t^2)$$

using Lemma 4.3.

By definition from the full tableau,

$$\begin{aligned}\Phi_{k+1}^{(0)}(t) &= \Phi_k^{(0)}(t)\,[\overline{\Phi_k^{(0)}(t)}\Phi_k^{(1)}(t)]^t \\ &= S_0[1 + kt\log(\overline{S_0}S_1) + O(t^2)][1 + t\log(\overline{S_0}S_1) + O(t^2)] \\ &= S_0[1 + (k+1)t\log(\overline{S_0}S_1) + O(t^2)]\end{aligned}$$

as required. □

Putting these results for additive and multiplicative motions together gives the following theorem.

Theorem 4.5. *If $S(t)$ is a Bézier motion of degree n defined by the control poses S_i, for $0 \le i \le n$, then*

(i) in the additive case, the derivatives at the ends of the segment are given as

$$\dot{S}(0) = n(S_1 - S_0), \quad \dot{S}(1) = n(S_n - S_{n-1});$$

(ii) in the multiplicative case, the derivatives at the ends of the segment are given as

$$\dot{S}(0) = nS_0\log(\overline{S_0}S_1), \quad \dot{S}(1) = -nS_n\log(\overline{S_n}S_{n-1}).$$

Proof. For the end of the segment at $t = 0$, the theorem follows from Lemmas 4.2 and 4.4. The result for the end at $t = 1$ is proved by noting that by reordering the control poses in the de Casteljau tableau

$$S_{0,1,\ldots,n}(t) \;=\; S_{n,n-1,\ldots,0}(1-t).$$

□

The result can also be expressed in terms of values of the velocity indicatrix.

Corollary 4.6. *If $S(t)$ is a Bézier motion of degree n defined by the control poses S_i, for $0 \le i \le n$, then*

(i) in the additive case, the velocity indicatrices at the ends of the segment are given by

$$\begin{aligned} \Psi(0) &= 2nS_0^{-1}(S_1 - S_0), \\ \Psi(1) &= 2nS_n^{-1}(S_n - S_{n-1}); \end{aligned} \tag{20}$$

(ii) in the multiplicative case, the velocity indicatrices at the ends of the segment are given by

$$\begin{aligned} \Psi(0) &= 2n\log(\overline{S_0}S_1), \\ \Psi(1) &= -2n\log(\overline{S_n}S_{n-1}). \end{aligned} \tag{21}$$

Proof. This follows from the definition of the velocity indicatrix in (11). □

Two motion segments are said to join with C^1-continuity if the motions and the linear and angular velocities are continuous across the join. A necessary and sufficient condition for the constraint on velocities is that the velocity indicatrix is either continuous across the join or only suffers a jump discontinuity which is a pseudoscalar.

If a motion segment is to be joined with C^1-continuity to the end of a given segment, then the first control pose S_0 of the new segment must be the final pose of the given segment. The final velocity indicatrix Ψ of the given segment determines the second control pose S_1 of the new segment via (20) or (21).

By analogy with free-form curves, the join has G^1-continuity if the motion itself is continuous and the linear and angular velocities on either side are

the same multiple of each other. If a second segment is joined to an existing one, so that the velocity indicatrix Ψ_0 at the existing end is known, then the relation determining S_1 becomes the following. The corresponding relation for S_{n-1} at the other end of the segment is also given; it is assumed that S_0 and S_n are both unitary

$$\begin{aligned} \text{additive:} \qquad S_1 &= S_0[1 + \tfrac{1}{2n}(\lambda_0 \Psi_0 + \gamma_0)], \\ S_{n-1} &= S_n[1 - \tfrac{1}{2n}(\lambda_n \Psi_n + \gamma_n)], \end{aligned} \tag{22}$$

$$\begin{aligned} \text{multiplicative:} \qquad S_1 &= S_0 \exp\left(\tfrac{1}{2n}(\lambda_0 \Psi_0 + \gamma_0)\right), \\ S_{n-1} &= S_n \exp\left(-\tfrac{1}{2n}(\lambda_n \Psi_n + \gamma_n)\right). \end{aligned} \tag{23}$$

The scalar factor λ_0 and the pseudoscalar γ_0 introduce additional choice for the control poses at the start of a motion segment. A similar factor λ_n and pseudoscalar γ_n can be used at the other end. Such factors maintain the intrinsic derivative constraints of the motion in a manner equivalent to geometric shape factors in curve design [16], although C^1-continuity is lost.

This section concludes with an example to illustrate some of the ideas, particularly for additive motions. The top part of Fig. 3 shows a planar motion formed of two additive cubic segments: one is around a quadrant of a circle; the other is along a straight line. The poses of a cuboidal block during the motion are shown, together with the path traced by the centre of the block. The control points for the arc are

$$\begin{aligned} U_0 &= 0.7071 + 0.7071 e_{12} \\ U_1 &= 0.8047 + 0.4714 e_{12} + 0.6667 e_{1\infty} + 0.6667 e_{2\infty} \\ U_2 &= 0.9024 + 0.2357 e_{12} + 1.3333 e_{1\infty} + 1.3333 e_{2\infty} \\ U_3 &= 1.0000 + 2.0000 e_{1\infty} + 2.0000 e_{2\infty} \end{aligned}$$

and those along the straight line

$$\begin{aligned} V_0 &= 1.0000 + 2.0000 e_{1\infty} + 2.0000 e_{2\infty} \\ V_1 &= 1.0000 + 3.0472 e_{1\infty} + 2.0000 e_{2\infty} \\ V_2 &= 1.0000 + 4.0944 e_{1\infty} + 2.0000 e_{2\infty} \\ V_3 &= 1.0000 + 5.1416 e_{1\infty} + 2.0000 e_{2\infty}. \end{aligned}$$

The distances travelled by the centre of the block in the two parts of the motion are the same. Each part is over an interval of size 1 for the parameter t, so that the complete motion is over the interval $0 \leq t \leq 2$.

The graphs in Fig. 3 show the linear (for the centre of the cuboid) and angular speeds during the motion. These are not constant over the the quadrant since the additive motion is not at constant speed there. Naturally, both graphs are discontinuous where the motion changes form.

The velocity indicatrix at the end of the quadrant is

$$\Psi \;=\; 0.5858 - 1.4142e_{12} + 5.6569e_{2\infty}.$$

Continuity of velocity can be achieved by replacing control pose V_1 by

$$V_1 \;=\; V_0[1 + \tfrac{1}{6}(\Psi + \gamma)]$$

where γ is a pseudoscalar.

Fig. 4 shows the effect of taking γ to be zero, ± 5, and ± 10. In each case, the motion remains planar. The upper part of the figure shows the path of the centre of the cuboid, and the graphs show the corresponding linear and angular speeds. The positive values have the effect of "straightening" the curve around the join but this is at the expense of making the speeds less smoothly varying. Negative values distort the path considerably.

Fig. 5 compares the case $\gamma = 0$ with when $\gamma = \pm 20\omega$, and $\gamma = \pm 40\omega$. The main effect is to take the motion out of the plane. The top part of the figure shows the paths viewed along the y-axis; the views along the z-axis are identical to the $\gamma = 0$ case in Fig. 4. This increases the linear speed as shown in the graph in Fig. 5; the angular speed in all cases is the same as that for $\gamma = 0$ in Fig. 4.

5. Examples

Three examples of motions are discussed in this section.

5.1. Motion construction from given end-conditions

The following constraints are taken from Belta and Kumar [4] where motions are constructed using matrix-based techniques. The end poses are specified in terms of: the position vector $\mathbf{r}$ of the reference point in the moving body, a unit vector $\mathbf{a}$ giving the direction of the axis of rotation, and the angle θ (in radians) of the rotation about that axis. The speeds are specified by the velocity $\mathbf{v}$ of the reference point and the angular velocity vector $\boldsymbol{\Omega}$ of the body. Subscripts 0 and 3 are used for the start and finish of the motion.

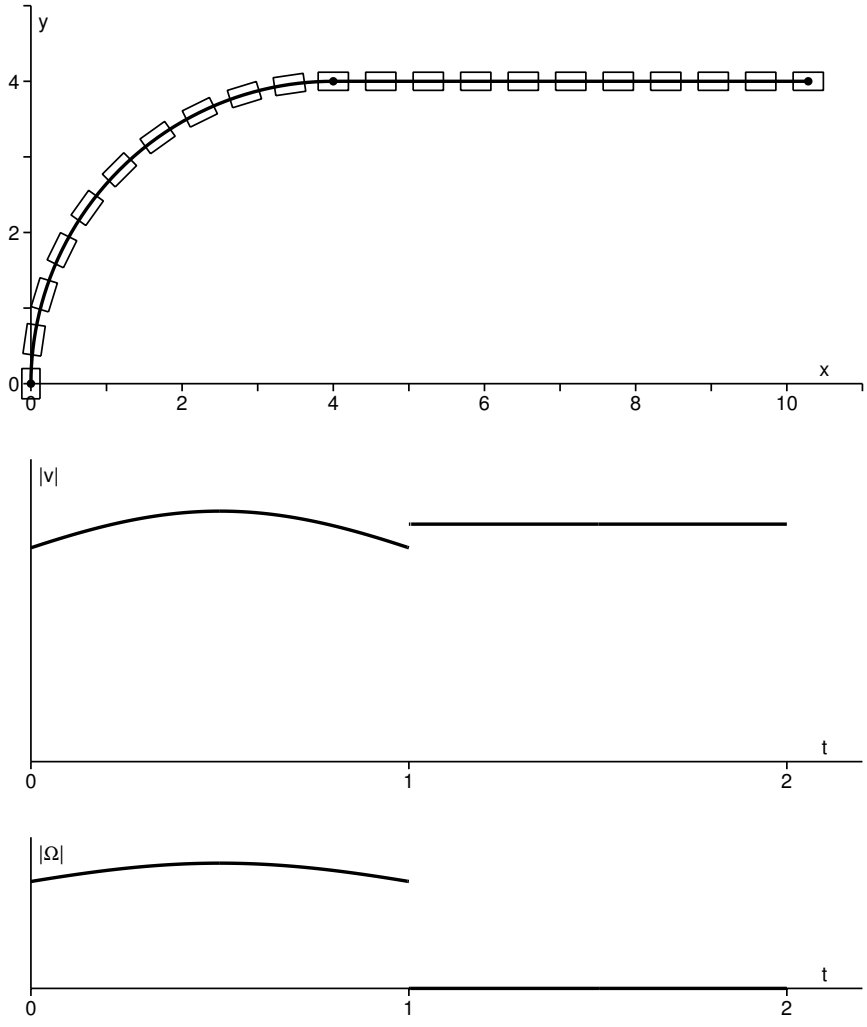

Figure 3: Motion formed of quadrant and straight line with linear and angular velocity graphs

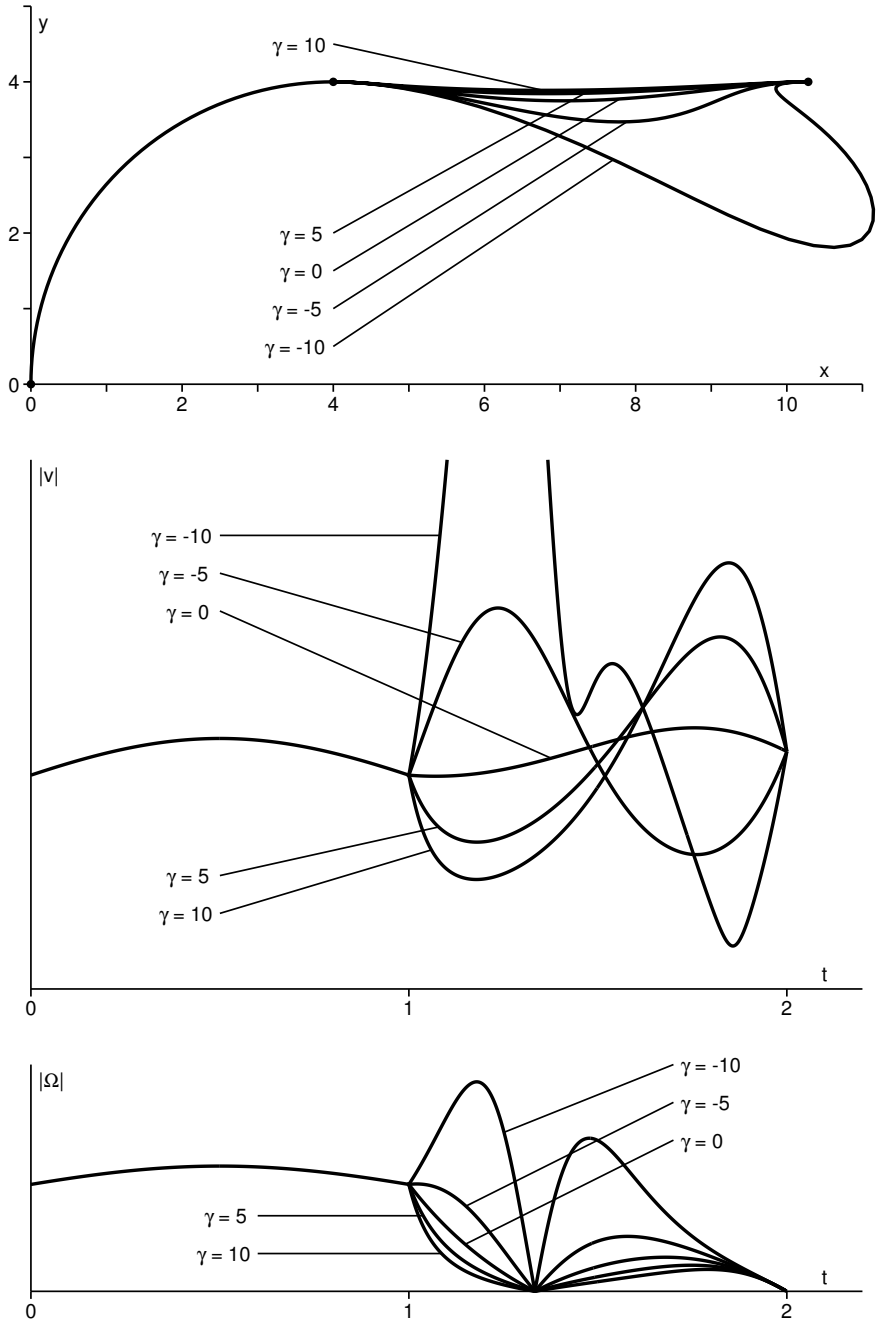

Figure 4: Modified motion and velocity graphs with γ real

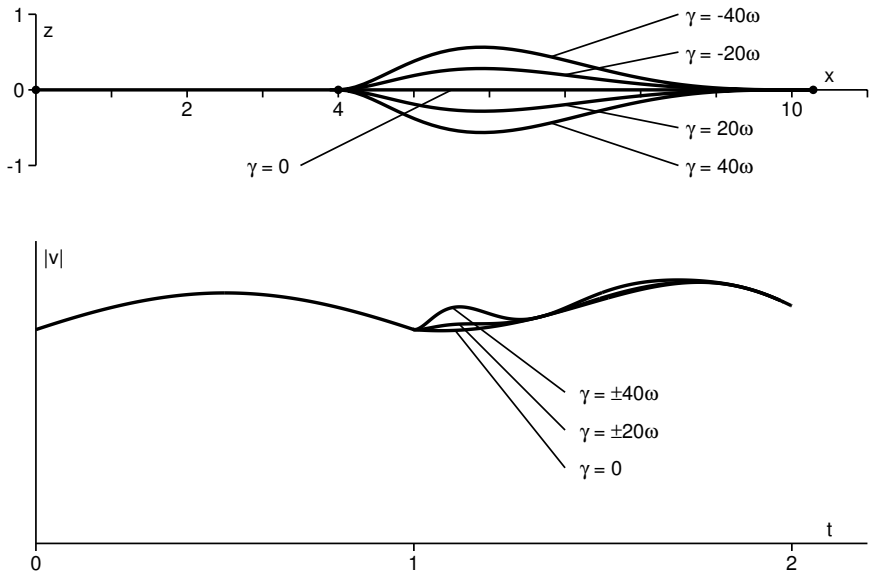

Figure 5: Modified motion and linear velocity graph with γ a multiple of $\omega = e_{123\infty}$

$\mathbf{r}_0 = (0, 0, 0)$	$\mathbf{r}_3 = (8, 10, 12)$
$\mathbf{a}_0 = (0, 0, 1)$	$\mathbf{a}_3 = (0.267, 0.535, 0.802)$
$\theta_0 = 0$	$\theta_3 = 1.959$
$\mathbf{v}_0 = (1, 1, 1)$	$\mathbf{v}_3 = (1, 5, 3)$
$\mathbf{\Omega}_0 = (1, 2, 3)$	$\mathbf{\Omega}_3 = (2, 1, 1)$

A cubic motion segment is formed with control poses S_0, S_1, S_2, S_3, and the parameter in the interval $0 \leq t \leq 1$. The end poses can be constructed by applying an appropriate rotation followed by a translation.

$$S_0 = R_0 T_0, \qquad S_3 = R_3 T_3,$$

where

$$\begin{aligned} R_0 &= 1 \\ T_0 &= 1 \\ R_3 &= \cos(\tfrac{1}{2}1.959) + \sin(\tfrac{1}{2}1.959)[0.267e_{23} + 0.535e_{31} + 0.802e_{12}] \\ T_3 &= 1 + \tfrac{1}{2}[8e_{1\infty} + 10e_{2\infty} + 12e_{3\infty}]. \end{aligned}$$

Now (14) is used to determine the velocity u of the point in the body instantaneously at the origin (in particular, $u_0 = v_0$) and the rest of Theorem 3.2 gives the velocity bivector at the ends of the segment. The velocity indicatrix is taken to be the same as the velocity bivector.

For a multiplicative motion, (23) determines poses S_1, S_2.

The resultant control poses are as follows

$$\begin{aligned}
S_0 &= 1.000 \\
S_1 &= 0.812 + 0.468e_{12} - 0.312e_{13} + 0.156e_{23} \\
&\quad +0.147e_{1\infty} + 0.138e_{2\infty} + 0.129e_{3\infty} + 0.156\omega \\
S_2 &= 0.763 + 0.413e_{12} - 0.497e_{13} - 0.013e_{23} \\
&\quad +1.683e_{1\infty} + 1.508e_{2\infty} + 6.308e_{3\infty} + 4.363\omega \\
S_3 &= 0.557 + 0.666e_{12} - 0.444e_{13} + 0.222e_{23} \\
&\quad +2.895e_{1\infty} + 1.456e_{2\infty} + 4.010e_{3\infty} + 7.101\omega.
\end{aligned}$$

The cubic multiplicative motion obtained is shown in Fig. 6. Poses are shown using an L-shaped block.

For an additive motion, (21) determines poses S_1, S_2; poses S_0, S_3 remain unchanged.

$$\begin{aligned}
S_1 &= 1.000 + 0.500e_{12} - 0.333e_{13} + 0.167e_{23} \\
&\quad +0.167e_{1\infty} + 0.167e_{2\infty} + 0.167e_{3\infty} \\
S_2 &= 0.816 + 0.462e_{12} - 0.536e_{13} - 0.001e_{23} \\
&\quad +1.934e_{1\infty} + 1.764e_{2\infty} + 6.877e_{3\infty} + 4.707\omega.
\end{aligned}$$

The cubic additive motion obtained is shown in Fig. 7.

It is worth noting the additive motion appears similar to that of multiplicative interpolation. This property has been identified previously [17, 28] and suggests non-unitary motions can be utilised as effectively as unitary motions. Two potential advantages of non-unitary motions are the possibility of a simplified representation (polynomial expressions) and further possible degrees of freedom in the form of pseudoscalar modifications to the velocity indicatrices at the ends of a motion.

5.2. Scaling the velocity indicatrix

This example considers the effect of shape factors modifying the velocity indicatrix at either end of a motion segment. A planar motion is considered whose end conditions are based on the following constraints.

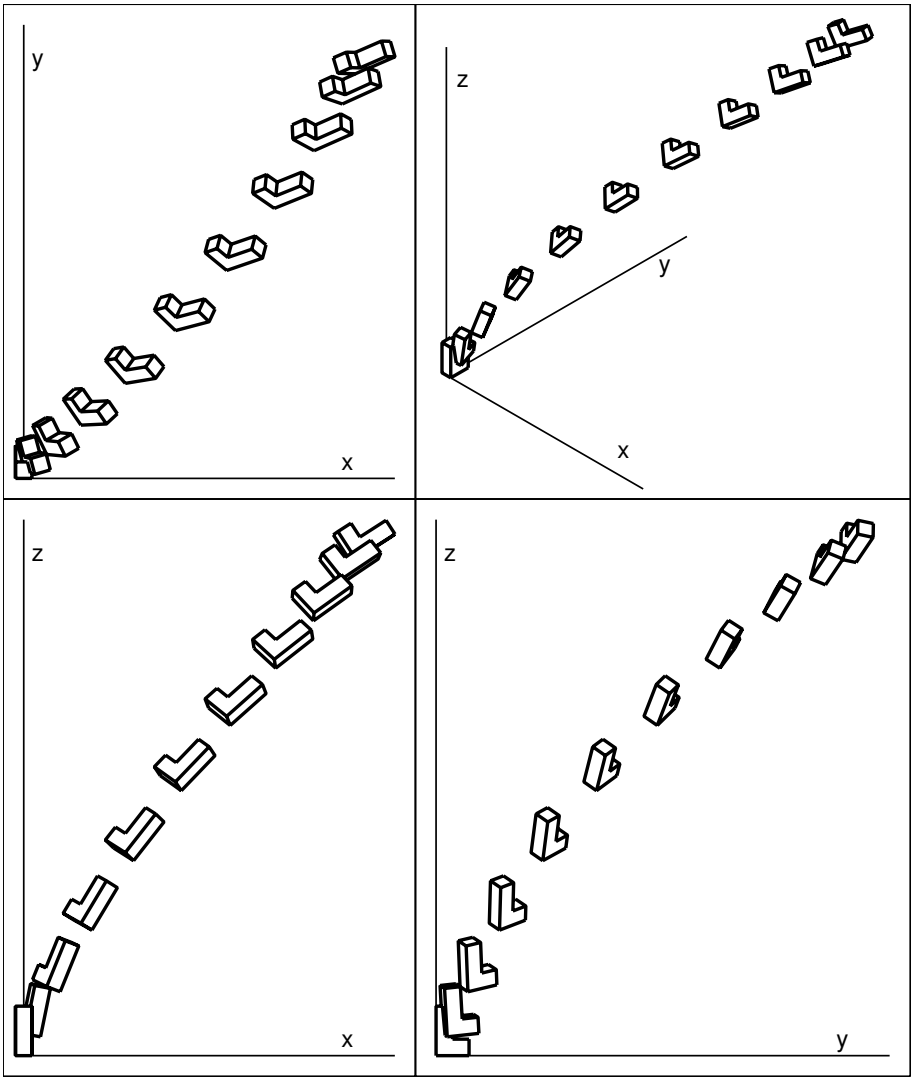

Figure 6: Multiplicative cubic motion

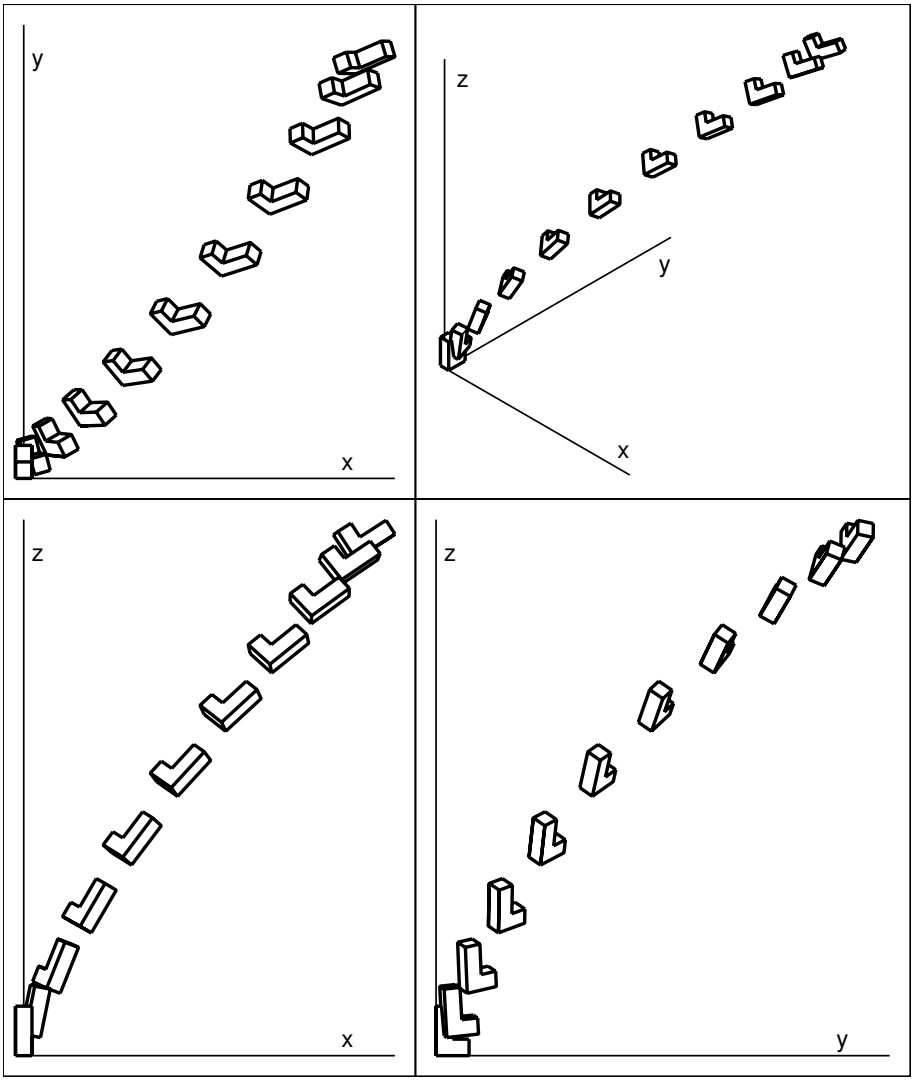

Figure 7: Additive cubic motion

$\mathbf{r}_0 = (0, 0, 0)$	$\mathbf{r}_3 = (0, 10, 0)$
$\mathbf{a}_0 = (1, 0, 0)$	$\mathbf{a}_3 = (1, 0, 0)$
$\theta_0 = 0$	$\theta_3 = -\frac{\pi}{2}$
$\mathbf{v}_0 = (0, 0, 8)$	$\mathbf{v}_3 = (0, 4, 0)$
$\mathbf{\Omega}_0 = (-\frac{\pi}{4}, 0, 0)$	$\mathbf{\Omega}_3 = (\frac{\pi}{8}, 0, 0)$

A cubic motion segment is again used with control poses S_0, S_1, S_2, S_3, with the parameter satisfying $0 \leq t \leq 1$.

As with the last example, the end poses are constructed as products of a rotation and a translation.

Using (14), the end constraints give the following values for the velocity bivector at the ends of the segment

$$\begin{aligned} \nu_0 &= -0.785e_{23} + 8.000e_{3\infty} \\ \nu_3 &= 0.393e_{23} + 4.000e_{2\infty} - 3.927e_{3\infty}. \end{aligned}$$

The values for the velocity indicatrix at the ends of the segment are taken to be

$$\Psi_0 = \lambda_0(\nu_0 + \gamma_0), \qquad \Psi_3 = \lambda_3(\nu_3 + \gamma_3),$$

where λ_0, λ_3 are scalar shape factors, and γ_0, γ_3 are pseudoscalars. The values used for the latter are arbitrarily chosen as

$$\gamma_0 = \tfrac{1}{2} + \tfrac{1}{2}\omega, \qquad \gamma_3 = 1 - \tfrac{1}{2}\omega.$$

Control poses S_1, S_2 can then be determined using (22) and (23).

The cubic multiplicative motion obtained is shown in Fig. 8 for the shape factors λ_0 and λ_3 taking the values 1 and 4 (where 1 is the default choice and 4 is an arbitrary alternative value). The control pose S_1 is given by (22) in which the variables are fixed apart from λ_0. Hence, as λ_0 varies, S_1 represents an additive Bézier motion of degree 1. Generally when such a motion is applied to a body, each point in the body moves around the surface of a circular cylinder (with a common axis) along a planar path which is therefore an ellipse [29]. This is a vertical Darboux motion [13, 30]. This also applies to S_2. As this example is planar, the movements related to the middle control poses are along circular arcs, shown as dashed curves in the figure. The effect of changing the shape factor is comparable to the familiar effect in curve design where moving the second control point of a

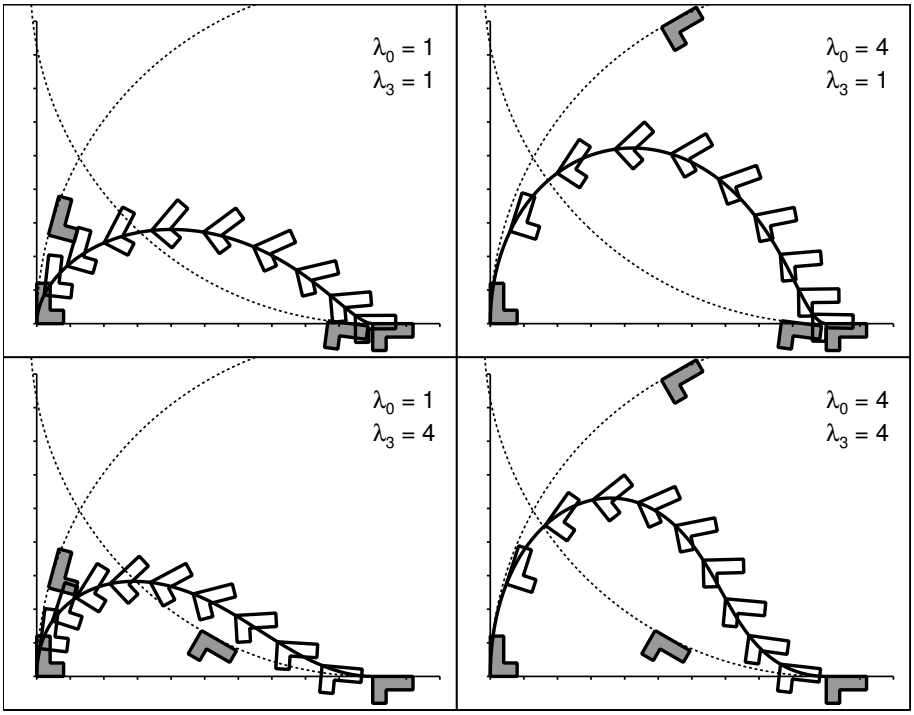

Figure 8: Multiplicative cubic motion varying shape factors

curve along the line joining it to the first control point leaves the direction of the end-tangent to the curve unchanged.

The numerical values for the control poses are as follows. In all cases, the end poses are

$$\begin{aligned} S_0 &= 1.000 \\ S_3 &= 0.707 - 0.707e_{23} + 3.536e_{2\infty} + 3.536e_{3\infty}. \end{aligned}$$

The other control poses depend upon the corresponding shape factor.

$$\begin{aligned} \lambda_0 = 1: \; S_1 &= 1.078 - 0.142e_{23} + 0.012e_{1\infty} + 1.445e_{3\infty} + 0.090\omega \\ \lambda_0 = 4: \; S_1 &= 1.209 - 0.698e_{23} + 0.233e_{1\infty} + 7.108e_{3\infty} + 0.403\omega \\ \lambda_3 = 1: \; S_2 &= 0.558 - 0.636e_{23} + 0.053e_{1\infty} + 2.392e_{2\infty} + 2.783e_{3\infty} + 0.047\omega \\ \lambda_3 = 4: \; S_2 &= 0.257 - 0.445e_{23} + 0.148e_{1\infty} + 0.326e_{2\infty} + 1.266e_{3\infty} + 0.086\omega. \end{aligned}$$

The corresponding cubic additive motion is given in Fig. 9 for the same shape factors. These have the same effect as in the multiplicative case.

Note that there is now a greater difference between the additive and multiplicative motions for a given set of control poses than there is in the previous example. This is due to choosing non-zero pseudoscalars γ_0 and γ_3.

The end control poses are as before. The other two poses take the following values.

$$\begin{aligned} \lambda_0 = 1: \; S_1 &= 1.083 - 0.131e_{23} + 1.333e_{3\infty} + 0.083\omega \\ \lambda_0 = 4: \; S_1 &= 1.333 - 0.524e_{23} + 5.333e_{3\infty} + 0.333\omega \\ \lambda_3 = 1: \; S_2 &= 0.543 - 0.636e_{23} + 0.059e_{1\infty} + 2.243e_{2\infty} + 2.706e_{3\infty} + 0.059\omega \\ \lambda_3 = 4: \; S_2 &= 0.051 - 0.421e_{23} + 0.236e_{1\infty} - 1.633e_{2\infty} + 0.218e_{3\infty} + 0.236\omega. \end{aligned}$$

5.3. Hermite interpolation

This example is based on a motion considered by Jaklič et al. [3]. It is specified in terms of the path traced by a reference point in the moving body given, using the geometric algebra notation, by

$$c(t) = e_0 + [3\log(t+1)\cos t]e_1 + [3\log(t+1)\sin t]e_2 + 3(t+1)e_3,$$

and the rotation of the body about this point given by the following quaternion (again expressed in geometric algebra form)

$$q(t) = t + [t + \cos\tfrac{\pi}{4}t]e_{23} + [\sin\tfrac{\pi}{4}t]e_{31} + [\cos\tfrac{\pi}{10}t]e_{12}.$$

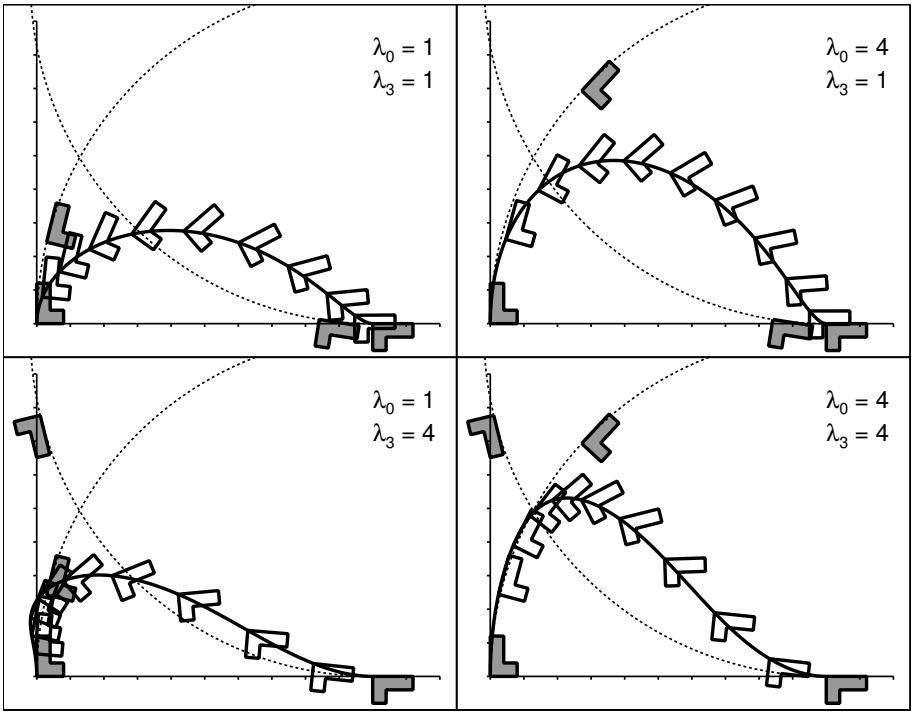

Figure 9: Additive cubic motion varying shape factors

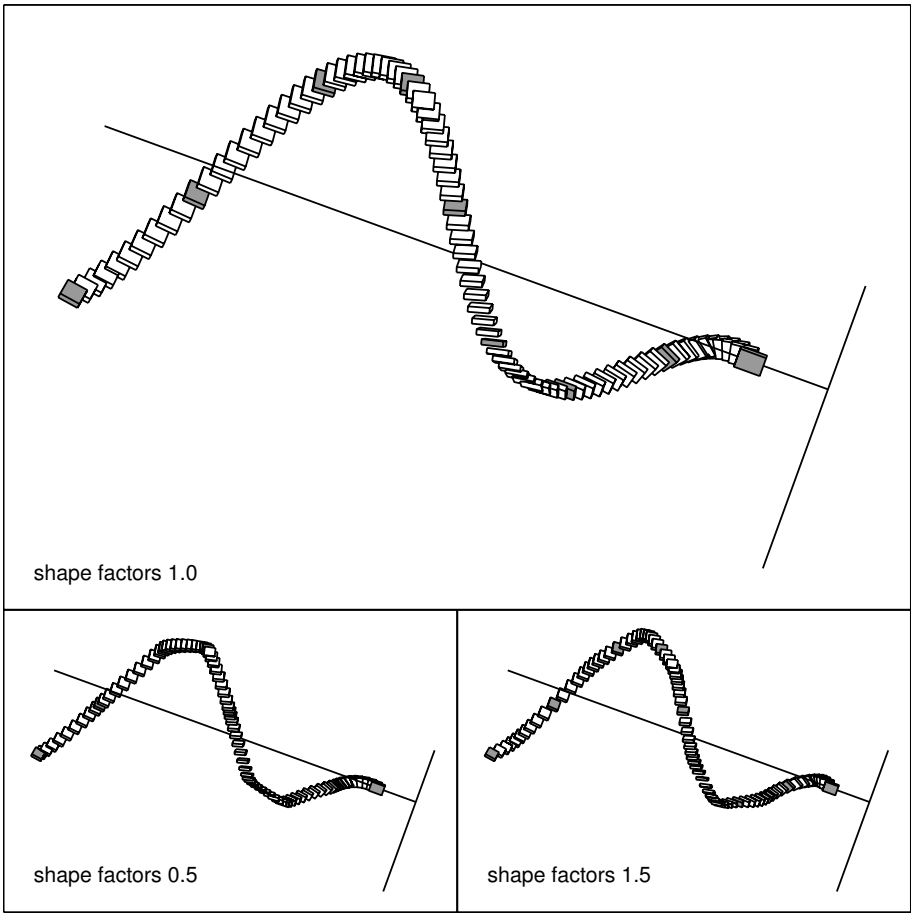

Figure 10: Hermite interpolation of an additive cubic motion through nine precision poses with different (common) values for the shape factors

The motion [3] is considered between $t = 1$ and $t = 9$, splitting it into eight segments with the divisions at integer values of t. The above relations allow the pose (position and orientation) to be found at each division along with the linear and angular velocities (treating the parameter t as time).

What is done here is to use Theorem 3.2 to form the velocity bivector and indicatrix (taking the pseudoscalar $\gamma(t)$ to be zero) at each division. A motion for each segment is then formed as a cubic segment using the known end poses as the first and last control poses and (22) or (23) to form the other two control poses.

The resultant additive motion is shown in the upper part of Fig. 10. This is taking all the shape factors as unity. The shaded blocks are the poses at the ends of the segments. The construction ensures C^1-continuity between the segments.

The figure also shows the additive motions when the shape factors remain all the same but with different common values. When that value is 0.5, the effect is that the motion moves more quickly away from the segments ends making the motion turn more sharply at each join and be flatter between the joins. When the common value is 1.5, the reverse is true: the motion is flatter across the joins and turns sharply in the middle of each segment.

The construction ensures that the motion remains C^1-continuous in both of these two revised cases. Other motions can be created by taking any combination of segments from the three cases. Such combinations are G^1-continuous across the joins.

6. Conclusions

This paper has considered free-form motions created via the use of geometric algebra. The conformal geometric algebra (CGA) has been used but similar approaches can be adopted with other versions of geometric algebra. A motion is constructed as a parametric function from a number of specified control poses using the de Casteljau algorithm. Its definition is independent of any choice of reference point in the body.

The construction requires the ability to combine two poses to produce another pose. One combination makes use of the slerp (spherical linear interpolation) operation. This forms the product of powers of poses and the resultant motion is here called multiplicative. If the original control poses are all unitary then each pairwise combination is also unitary including therefore the resultant motion itself. In the unitary case, forming the derivative

of the motion with respect to the parameter allows the velocity bivector to be formed and this holds information about the linear and angular velocities of a body undergoing the motion.

An alternative form of combination has been seen to be possible, one that uses linear interpolation between two poses. The result is an additive motion. This is no longer necessarily unitary and the theory regarding the derivative has been extended. The previous construction now yields the velocity indicatrix which is the sum of the velocity bivector and a pseudoscalar.

Two motion segments join together with C^1-continuity if the motion itself is continuous and the velocity bivector is also continuous. It is G^1-continuous if the velocity bivector at one side of the join is a scalar multiple of the velocity bivector on the other side. If pose and velocity conditions for the end of a segment are specified, then the end control pose is determined and so is the next pose along. If the interest is in gaining G^1-continuity between segments then there is some additional freedom in selecting that next pose. If additive motions are used, then there is still more freedom with the ability to adjust the pseudoscalar in the velocity indicatrix while leaving the velocity bivector unchanged.

This means that a range of motions that interpolate given precision poses can be obtained using Hermite cubic segments provided the linear and angular velocities at the precision poses are specified or can be selected in a suitable way.

References

[1] C. de Boor, K. Hollig, M. Sabin, High accuracy geometric Hermite interpolation, Comput. Aided Geom. Design 4 (4) (1987) 269–278.

[2] B. Cross, R. J. Cripps, Efficient robust approximation of the generalised Cornu spiral, J. Comput. Appl. Math. 273 (2015) 1–12.

[3] G. Jaklič, B. Jüttler, M. Kranj, V. Vitrih, E. Žagar, Hermite interpolation by rational G^k motions of low degree, J. Comput. Appl. Math. 240 (2013) 20–30.

[4] C. Belta, V. Kumar, On the computation of rigid body motion, Elec. J. Comput. Kinematics 1 (2002) 1–12.

[5] M. Žefran, V. Kumar, Interpolation schemes for rigid body motions, Comput.-Aided Design 30 (3) (1998) 179–189.

[6] P. Crouch, G. Kun, F. Silva Leite, The de Casteljau algorithm on Lie groups and spheres, J. Dyn. Cont. Sys. 5 (3) (1999) 397–429.

[7] K. Shoemake, Animating rotation with quaternion curves, ACM SIGGRAPH Comput. Graph. 19 (3) (1985) 245–254.

[8] F. Allmendinger, S. Charaf Eddine, B. Corves, Coordinate-invariant rigid-body interpolation on a parametric C^1 dual quaternion curve, Mech. Mach. Theory 121 (2018) 731–744.

[9] O. Röschel, Rational motion design – a survey, Comput.-Aided Design 30 (3) (1998) 169–178.

[10] G. Leclercq, P. Lefèvre, G. Blohm, 3D kinematics using dual quaternions: theory and applications in neuroscience, Front. Behav. Neurosci. 7 (2013) 7:1–25.

[11] M. Pfurner, H.-P. Schröcker, M. Husty, Path planning in kinematic image space without the Study condition, in: Proceedings of Advances in Robot Kinematics 2016, J. Lenarčič, J.-P. Merlet, eds., Springer, Berlin, 2018

[12] A. Purwar, Q. J. Ge, On the effect of dual weights in computer aided design of rational motions, J. Mech. Design 127 (5) (2005) 967–972.

[13] A. Purwar, Q. J. Ge, Kinematic convexity of rigid body displacements, in: Proceedings of the ASME 2010 International Design Engineering Technical Conferences & Computer and Information in Engineering Conference IDETC/CIE 2010, Montreal, (2010) 1–12.

[14] J. Siegele, M. Pfurner, H.-P. Schröcker, Space kinematics and projective differential geometry over the ring of dual numbers, J. Geom. Graph., 25(1) (2021) 19–31.

[15] L. Kavan, S. Collins, J. Zara, C. O'Sullivan, Geometric skinning with approximate dual quaternion blending, ACM Trans. Graph. 27(4): (2008) 105:1–23.

[16] B. A. Barsky, T. D. DeRose, Geometric continuity of parametric curves: three equivalent characterizations, IEEE Comput. Graph. Appl. 9 (6) (1989) 60–68.

[17] M. Hunt, G. Mullineux, R. J. Cripps, B. Cross, Free-form additive motions using conformal geometric algebra, Proc. Instn Mech. Engrs – Part C: J. Eng. Sci. 232 (9) (2018) 1560–1571.

[18] G. Mullineux, R. J. Cripps, B. Cross, Bézier motions with end-conditions of speed, Comput.-Aided Design 63 (2018) 135–148.

[19] C. Cibura, L. Dorst, Determining conformal transformations in R^n from minimal correspondence data, Math. Meth. Appl. Sci. 34 (2011) 2031–2046.

[20] J. M. Selig, Clifford algebra of points, line and planes, Robotica (2000) 18 (5) 545–556.

[21] R. González Calvet, Treatise of plane geometry through geometric algebra, Cardanyola del Vallés, TIMSAC, 2007.

[22] C. Gunn, On the homogeneous model of Euclidean geometry, in: Guide to Geometric Algebra in Practice, Dorst L and Lasenby J, eds. Springer-Verlag, 2011, pp. 297–327.

[23] F. Beer, E. Johnson, P. Cornwell, B. Self, Vector Mechanics for Engineers: Dynamics, 12th edition, McGraw-Hill, 2019.

[24] J. M. McCarthy, G. S. Soh, Geometric Design of Linkages, 2nd edition, Springer, 2011.

[25] G. Farin, Curves and Surfaces for CAGD: A Practical Guide, 5th edition, Morgan Kaufmann, 2002.

[26] K. Počkaj, Hermite G^1 rational spline motion of degree six, Numer. Algorithms 66 (2014) 721–739.

[27] M. Krajnc, Interpolation with spatial rational Pythagorean-hodograph curve of class 4, Comput. Aided Geom. Design 56 (2017) 16–34.

[28] R. J. Cripps, G. Mullineux, Constructing 3D motions from curvature and torsion profiles, Comput.-Aided Design 44 (5) (2012) 379–387.

[29] G. Mullineux, L. Simpson, Rigid-body transforms using symbolic infinitesimals, in: Guide to Geometric Algebra in Practice, L. Dorst, J. Lasenby (eds.), Springer-Verlag, 2011, 353–369.

[30] O. Bottema, B. Roth, Theoretical Kinematics, Dover Publications, 1979.

Appendix 1: proof of Lemma 2.2

One of the difficulties in dealing with the algebra $\mathcal{G}_{0123\infty}$ is that the rule "the reverse of a product is the product of the reverses in the other order" does not apply. However, it does apply for the algebra $\mathcal{G}_{123\infty}$. So if the vector x in the statement of Lemma 2.2 lies in $\mathcal{G}_{123\infty}$, then $\overline{S}xS$ is an element of odd grade which is equal to its own reverse. Hence it is a vector and this proves part (i) of the lemma (with $\lambda = 0$).

More generally, x has the form $\gamma e_0 + v$ where γ is a real coefficient and $v \in \mathcal{G}_{123\infty}$ is a vector. Then

$$\overline{S}xS = \gamma \overline{S}e_0 S + \overline{S}vS.$$

Hence by the previous remark, it is sufficient to prove part (i) when $x = e_0$.

The form of the even-grade element S is

$$S = \xi + ae_\infty + b + \eta\omega$$

where ξ, η are real numbers, and $a, b \in \mathcal{G}_{123}$ are a vector and a bivector respectively. Then

$$\begin{aligned} \overline{S} &= \xi - ae_\infty - b + \eta\omega \\ e_0 S &= \xi e_0 + e_0 a e_\infty + e_0 b + \eta e_0 \omega. \end{aligned}$$

Now consider the products of each of the summands forming $\overline{S}$ with $e_0 S$, making use of (2) which is

$$e_\infty e_0 = -2 - e_{0\infty}$$

and the following relation derived from it

$$\omega e_0 = -2e_{123} + e_{0123\infty}.$$

$$\begin{aligned}
\xi e_0 S &= \xi^2 e_0 + \xi e_0 a e_\infty + \xi e_0 b + \xi\eta e_{0123\infty},\\
\\
-a e_\infty e_0 S &= -\xi a e_\infty e_0 - a e_\infty e_0 a e_\infty - a e_\infty e_0 b - \eta a e_\infty e_0 \omega\\
&= 2\xi a + \xi a e_0 e_\infty + 2a^2 e_\infty + a e_0 e_\infty a e_\infty\\
&\qquad +2ab + a e_0 e_\infty b + 2\eta a\omega + \eta a e_0 e_\infty \omega\\
&= 2\xi a - \xi e_0 a e_\infty + 2a^2 e_\infty + 2ab - e_0 a b e_\infty + 2\eta a\omega,\\
\\
-b e_0 S &= -\xi e_0 b - e_0 b a e_\infty - e_0 b^2 - \eta e_0 b\omega,\\
\\
\eta\omega e_0 S &= \xi\eta\omega e_0 + \eta\omega e_0 a e_\infty + \eta\omega e_0 b + \eta\omega e_0\omega\\
&= -2\xi\eta e_{123} + \xi\eta e_0\omega - 2\eta e_{123} a e_\infty + \eta e_0\omega a e_\infty\\
&\qquad -2\eta e_{123} b + \eta e_0\omega b - 2\eta^2 e_{123}\omega + \eta^2 e_0\omega^2\\
&= -2\xi\eta e_{123} + \xi\eta e_{0123\infty} - 2\eta a\omega - 2\eta b e_{123} + \eta e_0 b\omega + 2\eta^2 e_\infty.
\end{aligned}$$

Adding these, and noting that $ab = (a\cdot b) + (a\wedge b)$, gives

$$\begin{aligned}
\overline{S} e_0 S &= (\xi^2 - b^2)e_0 + 2\xi a - 2\eta b e_{123} + 2(a\wedge b) + 2(a^2+\eta^2)e_\infty\\
&\qquad +2(a\cdot b) - e_0(ab+ba)e_\infty - 2\xi\eta e_{123} + 2\xi\eta e_{0123\infty}\\
\\
&= [(\xi^2 - b^2)e_0] + 2[\xi a - \eta b e_{123} + (a\wedge b)] + 2[(a^2+\eta^2)e_\infty]\\
&\qquad +2[(a\cdot b) - \xi\eta e_{123}] - 2e_0[(a\cdot b) - \xi\eta e_{123}]e_\infty.
\end{aligned}$$

The inner product $a\cdot b$ is a scalar multiple of e_{123}. Suppose that λ is the real number such that

$$2[(a\cdot b) - \xi\eta e_{123}] \;=\; -\lambda e_{123}$$

and then, with $\sigma = -e_{123} + e_{0123\infty}$,

$$\overline{S} e_0 S = [(\xi^2 - b^2)e_0] + 2[\xi a - \eta b e_{123} + (a\wedge b)] + 2[(a^2+\eta^2)e_\infty] + \lambda\sigma. \quad (24)$$

Here, the first three terms in square brackets are all vectors. Hence $\overline{S} e_0 S$ has the required form.

For part (ii), multiplying out the terms shows that

$$\overline{S} S \;=\; (\xi^2 - b^2) - 2(a\cdot b)e_\infty + 2\xi\eta\omega$$

and hence has the required form with $\alpha = \xi^2 - b^2$. This is also the coefficient of e_0 in the expression of $\overline{S}e_0S$ in (24) and the latter part of (ii) follows.

It is sufficient for part (iii) to show that σ commutes with the basis vectors. This is immediate for e_1, e_2, e_3 as these commute with each of the summands of σ. So consider the outer products of σ with e_0 and e_∞.

$$\begin{aligned} e_0 \wedge \sigma &= \tfrac{1}{2} e_0 \wedge (e_0\omega + \omega e_0) \\ &= \tfrac{1}{4}(e_0e_0\omega + e_0\omega e_0 - e_0\omega e_0 - \omega e_0e_0) \\ &= 0, \end{aligned}$$

$$\begin{aligned} e_\infty \wedge \sigma &= \tfrac{1}{2} e_\infty \wedge (e_0\omega + \omega e_0) \\ &= \tfrac{1}{4}(e_\infty e_0\omega + e_\infty\omega e_0 - e_0\omega e_\infty - \omega e_0e_\infty) \\ &= \tfrac{1}{4}(e_\infty e_0\omega - \omega e_0e_\infty) \\ &= \tfrac{1}{4}((-2 - e_0e_\infty)\omega - e_{123}(-2 - e_0e_\infty)e_\infty) \\ &= \tfrac{1}{4}(-2\omega + 2e_{123}e_\infty) \\ &= 0. \end{aligned}$$

This completes the proof.

Appendix 2: velocity indicatrix and dual quaternions

The purpose of this appendix is to convert the result of Theorem 3.2 and hence provide an equivalent expression in dual quaternion form. This is to allow comparison of the work here with the dual quaternion approach used by other researchers [11, 12, 13, 14].

An isomorphism between the even-grade elements of $\mathcal{G}_{123\infty}$ and the dual quaternions is defined by the following pairings of basis elements.

$$\begin{aligned} 1 &\longleftrightarrow 1 & \qquad \omega &\longleftrightarrow \varepsilon \\ e_{12} &\longleftrightarrow -k & \qquad e_{1\infty} &\longleftrightarrow \varepsilon i \\ e_{13} &\longleftrightarrow +j & \qquad e_{2\infty} &\longleftrightarrow \varepsilon j \\ e_{23} &\longleftrightarrow -i & \qquad e_{3\infty} &\longleftrightarrow \varepsilon k \end{aligned}$$

An outer product can be defined between any two dual quaternions d_1 and d_2 with

$$d_1 \wedge d_2 = \tfrac{1}{2}(d_1d_2 - d_2d_1).$$

In particular

$$i \wedge j = k, \qquad j \wedge k = i, \qquad k \wedge i = j.$$

Then for dual quaternions, Theorem 3.2 says that the velocity indicatrix is given by

$$\Psi(t) = \gamma(t) + \nu(t)$$

where

$$\begin{aligned} \gamma &= \alpha + \varepsilon\beta \\ \nu &= \varepsilon(u_1 i + u_2 j + u_3 k) - (\Omega_1 i + \Omega_2 j + \Omega_3 k). \end{aligned}$$

Here α and β are scalars, u_1, u_2, u_3 are the components of the linear velocity of the point in the moving body instantaneously at the global origin, and Ω_1, Ω_2, Ω_3 are the components of the angular velocity vector, and all these are functions of t.

If $q = 1 + \varepsilon(q_1 i + q_2 j + q_3 k)$ represents the point Q in the body instantaneously at the point (q_1, q_2, q_3) (relative to global axes) then its velocity from equation (14) is

$$\begin{aligned} v_Q &= \varepsilon(u_1 i + u_2 j + u_3 k) - q \wedge (\Omega_1 i + \Omega_2 j + \Omega_3 k) \\ &= \varepsilon(u_1 i + u_2 j + u_3 k) + \varepsilon(\Omega_1 i + \Omega_2 j + \Omega_3 k) \wedge (q_1 i + q_2 j + q_3 k) \end{aligned}$$

and this is immediately comparable with (13).